

## A 3D a-priori velocity model for South American platform

Carolina Rivadeneyra-Vera<sup>1</sup>, Yvonne Font<sup>2</sup>, Marcelo Bianchi<sup>1</sup>

<sup>1</sup>Instituto de Astronomia, Geofísica e Ciências Atmosféricas/USP, Brazil; <sup>2</sup>Geoázur Laboratory-Observatoire de la Côte d'Azur - Research Institute for Development (IRD), France

Copyright 2021, SBGf - Sociedade Brasileira de Geofísica

This paper was prepared for presentation during the 17<sup>th</sup> International Congress of the Brazilian Geophysical Society held in Rio de Janeiro, Brazil, 16-19 August 2021.

Contents of this paper were reviewed by the Technical Committee of the 17<sup>th</sup> International Congress of the Brazilian Geophysical Society and do not necessarily represent any position of the SBGf, its officers or members. Electronic reproduction or storage of any part of this paper for commercial purposes without the written consent of the Brazilian Geophysical Society is prohibited.

### Abstract

The use of 3D velocity models significantly improves the accuracy of epicenter location since it can better predict wave travel times. Nevertheless, most of the events registered by the Brazilian Seismographic Network (RSBR) are located using 1D velocity models that lead to larger uncertainties. We have built a 3D a-priori P-wave velocity model for the South American Platform, including the Central Andes area; based on local and regional structural information and average velocities. To test the model reliability, we relocated the well-known Aiquile 1998 earthquake (Bolivia) using 14 regional P-wave arrivals, mostly belonging to the Bolivian Network, obtaining successful results when compared to the ground truth location of this earthquake. We also satisfactorily relocate two other recent important events of the South American Platform with similar results.

### Introduction

The South American platform presents an important seismicity; in Brazil, yearly, it is observed at least two events of magnitude 4.0 mb and it is expected one magnitude 5 mb each five years (Bianchi et al., 2018). On the other hand, the central Andean region presents at least one event of magnitude 5 mb each year (International Seismological Centre, 2013). Most of these earthquakes are located regionally using 1D standard velocity models (e.g. IASP91, AK135) that do not permit any kind of correlation to the known local geological structures. Another model routinely used by the USP/RSBR is the 1D NewBR model, which tries to mimic regional travel times (Assumpção et al., 2010).

The use of 3D velocity models significantly improves the earthquake location in regional scale, mainly capturing velocity heterogeneities of the crust and upper mantle. The error in travel time prediction at regional scale when using 1D velocity models could exceed 8 seconds (Myers et al., 2010). Many studies have focused on relocating regional or local seismicity with regional and local 3D velocity models (Font et al., 2003; Wu et al., 2008; Lin, 2013; Nugraha et al., 2018).

Globally, Myers et al. (2010) developed the global 3D RSTT (Regional Seismic Travel Time) model, which considers the effects of the crust and upper mantle structure in regional travel times for Pn waves, showing

epicenter accuracies of 5 km or better in Eurasia and North Africa, when stations with a maximum distance of 15° are used.

In South America, the RSTT model (Myers et al., 2010) and the iLoc algorithm (Bondár and Storchak, 2011) were used to relocate the well-known Andean Aiquile, 1998 earthquake (Funning et al., 2005). The initial results so far obtained were not satisfactory, as shown in Figure 1, probably because the RSTT model is not yet calibrated for South America.

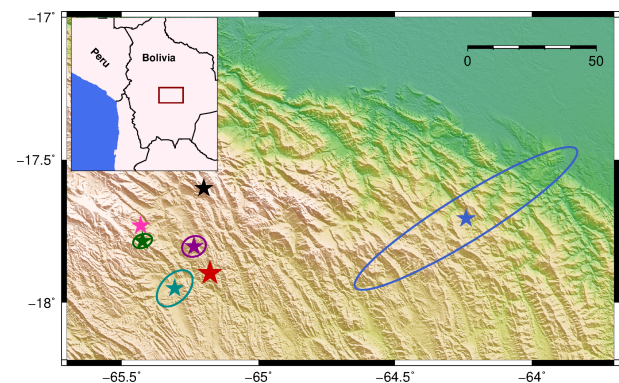


Figure 1: Relocation of Aiquile earthquake, 1998 (Bolivia) using the global 3D RSTT model (Myers et al., 2010). Red star: well-known epicenter determined by Funning et al. (2005). Epicenters given by different agencies: ISC (green star), NEIC (pink star) and Harvard (black star). Epicenter determined using stations up to 90° (blue star). Epicenter determined with stations corrected with the RSTT model up to 15° (turquoise star). Epicenter determined with stations up to 90° and corrected with the RSTT model up to 15° (purple star).

Due to the need to use 3D velocity models in event location we built one model for the stable region of South America, integrating structural information (topography, sediment basement and Moho depth) with velocity information for sediments, crystalline crust, and recent mantle 3D velocity profiles.

### Method

To facilitate the 3D model construction, we have taken into account the most important structural information at crustal scale. Since regional 3D velocity models obtained by different research groups so far do not cover our total area of interest, and neither have enough resolution in depth, we have constructed velocity laws from already published relevant data for the sediments and crust, and used a global model for the mantle velocities.

### Structural data

## 3D VELOCITY MODEL FOR THE SOUTH AMERICAN PLATFORM

We considered two first-order structures at crustal scale (sedimentary layer and the crystalline crust) that can be described by three interfaces:

- Topography/bathymetry surface from the ETOPO1 model (NOAA National Geophysical Center, 2009). This is a 1-arc minute global relief model of Earth's surface that integrates land topography and ocean bathymetry. In our study area, the topography varies from  $\sim 6$  km a.m.s.l. in the Andean region, to  $\sim 5$  km below the sea level in the oceanic area.
- Sedimentary basement interface: Knowing the role of sedimentary layer thickness in the epicenter location, we used the sediment information of CRUST1.0 model (Laske et al., 2013) in most parts of our study area. In the Paraná Basin a local available grid of depths was used.
- Moho discontinuity: Is the most important discontinuity at crustal scale because of its high velocity contrast and relevant depth variations. We used the updated crustal thickness map of South America from Rivadeneyra-Vera et al. (2019).

#### Sedimentary and Crustal velocities

To obtain the velocity laws, both for sediments and crust, we compiled velocity information from the literature, giving preference to active seismic experiments data because of its controlled accurate parameters (time and position). The predicted velocity law was obtained from fitting a polynomial regression to the averages of the researched bibliographic velocities.

The constructed velocity law for sediments (Figure 2), was obtained from velocity gradients of sedimentary basins around the world. We had no easy access to Brazilian regional scale data in a consistent manner. We opted for collect data from Los Angeles Basin (Süss and Shaw, 2003), the Indian Bengal Basin (Krishna and Rao, 2005; Damodara et al., 2017), Indian Palashi well (Murty et al., 2008), Norwegian-Danish Basin (Sandrin and Thybo, 2008), and Po Plain Basin in Italy (Molinari et al., 2015). The resulting velocity law varies between 1.7 km/s at the top of the sedimentary layer and goes up to 5 km/s at the bottom.

For crystalline crustal velocity law, we have considered two different tectonic areas:

- South American platform: we collected Brazilian available data of the central part (Soares et al., 2006) and northeast region (de Lima et al., 2019); we considered the average for platforms given by Christensen and Mooney (1995); and crustal velocity structures from global literature. The crustal velocity law obtained varies between 5.7 km/s and 7.1 km/s, without any variation from 37 km downwards.
- The Andes highlands: Considering the thicker crust under the Andes (up to  $\sim 70$  km), and the different velocity gradient due to their tectonic evolution (Beck and Zandt, 2002), we calculated another velocity law for this region, also considering the global average for orogens given by Christensen

and Mooney (1995), and active seismic studies in the region. The predicted velocity law ranges from 5.7 km/s to 7.1 km/s, and does not vary significantly below 40 km deep. It also considers the low velocity zone between 10 km and 20 km depth found in previous works.

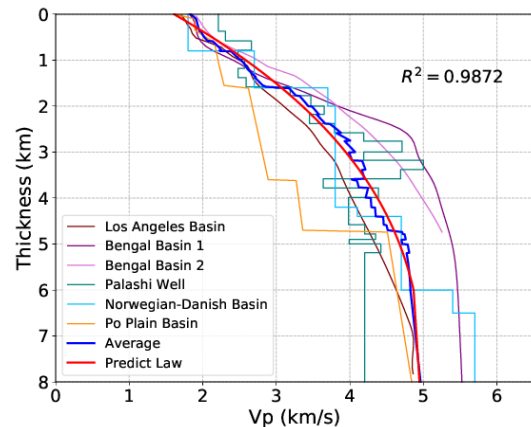


Figure 2: Velocity laws for the sediment layer. Blue line: average velocity of the collected data. Red curve: polynomial regression fit of the blue line.

Figure 3 compares the two different velocity laws for the crystalline crust. For the upper layers, both laws present very similar velocities; nevertheless, from 10 km down the Andean profile shows lower velocities, reaching the same velocity again at the bottom of each model, near the Moho discontinuity.

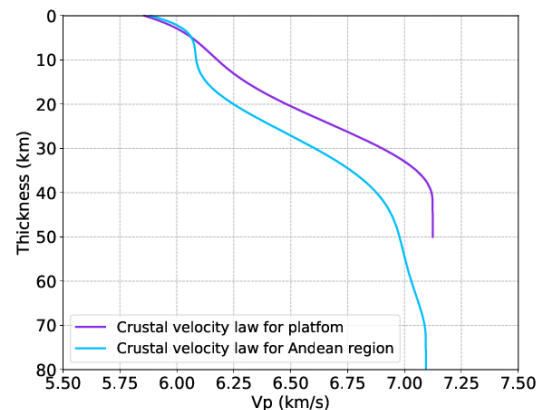


Figure 3: Comparison between velocity laws for platform and Andean region.

#### Mantle velocities

For the mantle, we used the LLNL-G3Dv3 global P-wave 3D velocity model (Simmons et al., 2012), which is heterogeneously distributed with a horizontal resolution of  $1^\circ$ . It is consistent with the global discontinuities at  $\sim 420$  and  $\sim 660$  km depth; and most important, with the position of the Nazca slab under the Andean and Sub-Andean region according to Portner et al. (2020). We sampled the mantle velocities and adjusted it at the upper mantle

position in our model, respecting the geographical position. The lowest mantle velocity is 7.8 km/s, mainly under the oceanic area, and the highest crustal velocity is ~7.1 km/s which ensures a consistent velocity jump at Moho discontinuity.

#### Parametrization and Model construction

We started our model at 7 km above sea level and extended it up to 900 km deep, considering that for regional distances (up to 30°) the theoretical rays do not go deeper than ~850 km, even for hypocenters deeper than 600 km (Kennett and Engdahl, 1991), as those of deep Andean earthquakes.

Considering the resolution of the available data, and the depth of our model; we defined a horizontal discretization of  $0.5^\circ \times 0.5^\circ$ , while the vertical discretization had different values depending on the depth: shallower than 10 km depth it is of 1 km due to the higher velocity gradient of the sediment velocity law; between 10 and 50 km, the resolution is of 2 km, and finally at mantle depths it is 5 km.

The area of interest (from 70°W to 34°W and from 32°S to 4°N) was divided into blocks of the size of horizontal and vertical discretization previously defined. Each block edge or node was used to represent the average velocity of the column below. As we have started the model at 7 km a.m.s.l. there are areas where there is only air, at these blocks the velocity was set at 0.3 km/s. When the topography relief begins we fill each node according to the structural information and velocity laws obtained. When one of the considered discontinuities (sediment basement or Moho depth) is between two nodes, the velocities of the two structure types were averaged.

The velocity laws for the platform and Andean region also were weighted, considering the distance of the node to both regions, in order to reduce any abrupt velocity change in two contiguous nodes.

#### Results

The 3D velocity model constructed contains 1 108 432 nodes. Figure 4 shows vertical cross-sections at 20°S, where lateral and depth velocity variations are observed. There is a clear velocity difference between the sediment layer, the crust, and mantle; without any depth velocity inversion in any structure. Lateral velocity variations are observed, depending on the presence of sedimentary basins (gray line), Moho depth (black line) and the distance to the Andean terranes. In the oceanic areas the mantle velocities are slightly lower than in continental areas. Black points represent nodes with velocities of 0.3 km/s as discussed.

The Andean region, characterized by a high topography, has a slightly lower velocity compared with the platform area, at the same depth; at the Nazca slab also there are smaller velocity changes. These variations are not noticeable due to the color scale used, which allows observing important velocity changes mainly at discontinuities.

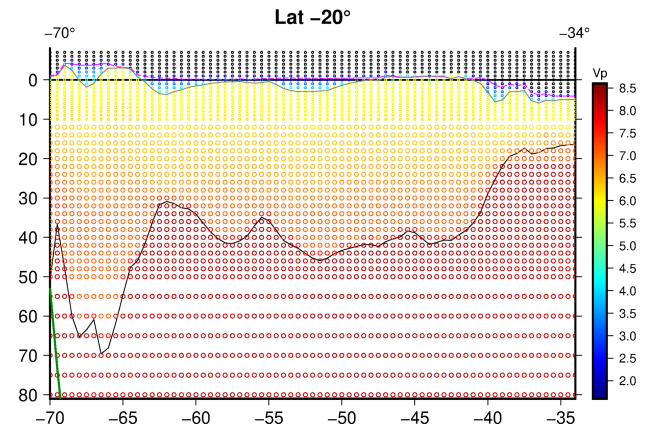


Figure 4: Vertical cross-section at 20°S, from 7km a.m.s.l. to 80 km depth. Fuchsia line: Topography relief. Gray line: Sediment basement. Black line: Moho depth. Green line: Nazca Slab. Black points represent nodes with velocities of 0.3 km/s as discussed in the text.

Figure 5 shows two horizontal cross-sections, the Andean region is delimited by a turquoise line and the continent-ocean margin by a green line. At 4 km depth, most of the continental area presents a crustal velocity of ~6 km while there are still noticeable lower sediment velocities (of ~4.5 km/s) in the Paraná Basin. As expected, the ocean region presents velocities corresponding to the sedimentary layer, being higher in areas closer to the continent.

The horizontal section at 36 km depth shows mainly crustal velocities of ~6.5 km/s in the continent; besides, the Sub-Andean and Pantanal Basin regions present mantle velocities, since these areas have a thinner crust (Rivadeneira-Vera et al., 2019).

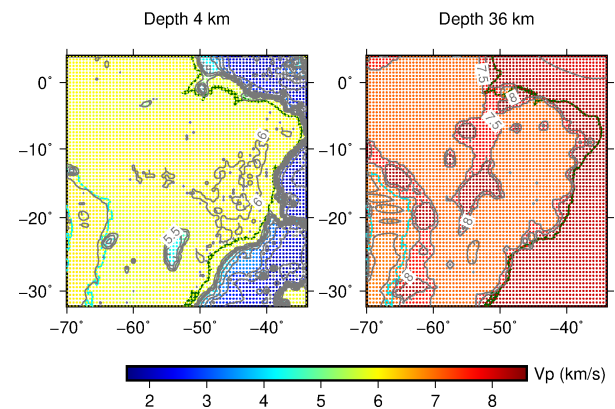


Figure 5: Horizontal section at 4 km and 36 km depth. Turquoise line: Andes limits. Green line: Continent-ocean margin. Grey lines: Velocity isolines.

#### Earthquakes location

To test our model we used the NonLinLoc (NNLoc) routine, developed by Lomax et al. (2009) that has been used satisfactorily in regional and local relocations using



## 3D VELOCITY MODEL FOR THE SOUTH AMERICAN PLATFORM

3D velocity models (Béthoux et al., 2016; Lomax, 2020). The NLLoc uses an efficient global sampling algorithm to obtain the a-posteriori probability density function (PDF) over possible solutions, quantifying the agreement between predicted and observed arrival times to all uncertainties, and forms a complete probabilistic solution.

We relocated the well-known Aiquile event using 14 P-wave arrivals, mostly belonging to the Bolivian network, located mainly in the Andean region. Figure 6 shows the relocation results, the semi-major axis of the error ellipsoid is about ~20 km, due to the fewer number of stations taken into account, being the closest one at  $-4^\circ$  away. Most of them are located to the west of the event, existing an important azimuthal gap in the east, and therefore a major error in this direction. Despite the large uncertainty, all stations considered have residuals less than 1 second, even the stations located in the Andean region that generally present higher residual values; the final RMS is 0.53 seconds. The obtained solution, using the proposed 3D model, is the closest one to the accurate epicenter given by Funning et al. (2005). One particularity of NLLoc is the fact that it returns two solutions, the Expected and the PDF. The PDF solution normally corresponds to the cloud average solution, while the Expected is the solution with the traditional best data missfit (lower RMS).

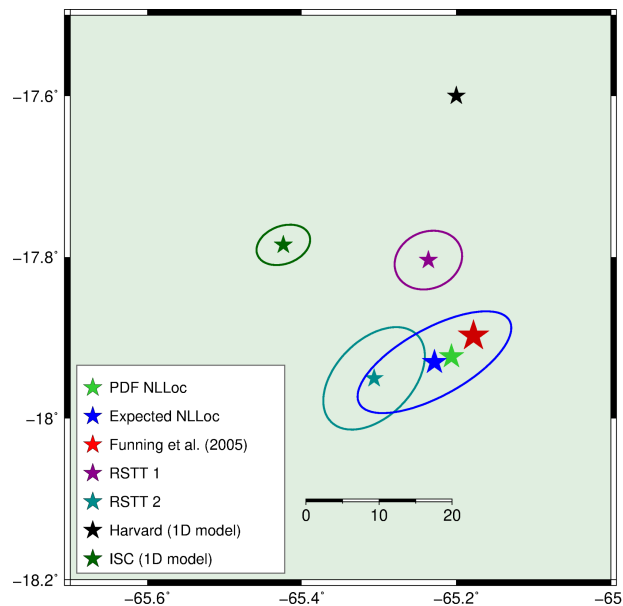


Figure 6: Aiquile relocation using the 3D velocity model and NonLinLoc routine. Epicenters given by international agencies are shown. RSTT 1: Epicenter determined with stations up to  $90^\circ$  and corrected with RSTT model up to  $15^\circ$ . RSTT 2: Epicenter determined with stations up to  $15^\circ$  corrected with RSTT model.

We also relocated other two recent important events that occurred at the South American stable platform. In both cases, our solution was satisfactory, showing a final RMS lower than 0.8 seconds when using stations up to  $15^\circ$ . The first event was the Amargosa 2020-08-30 10:44:28

UTC earthquake, located in northeast Brazil with a magnitude of 4,2 mR. This particular event had aftershocks well located by a local network (red stars in Figure 7). Also, using RSB data, two epicenters were obtained, one using the NewBR model with the Hypo71 routine (orange star) and the other, is the standard solution of the USP/RSBR, shown by the purple star.

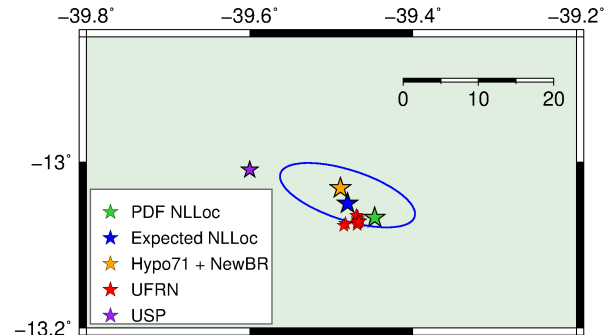


Figure 7: Amargosa earthquake relocation using the 3D velocity model and NLLoc routine (Blue and Green stars). Red stars are aftershocks well located by a local network operated by the UFRN.

Again in that specific case our solution was the closest solution to the known epicenter location. Right now we still can't properly solve the depths. On our tests we let the NLLoc sample a certain fixed depth range, normally correlated to the expected depth. We hope to be able to solve this issue when we incorporate S-wave velocities.

The last performed test was done using readings from the very recent Guayana 2021-01-31 19:05:13 UTC earthquake (Figure 8). This was the largest event (Mag. 5.7 mb) in the South American platform recorded by the Brazilian Seismographic Network so far. In this example, the large uncertainty in the north-east direction is due to the event being at the limit of our model, which limits the use of stations to the north of the event. Again, depths were hard to constrain and in this case our solution was similar to the USP/RSBR solution; considering the uncertainty given by the determined PDF.

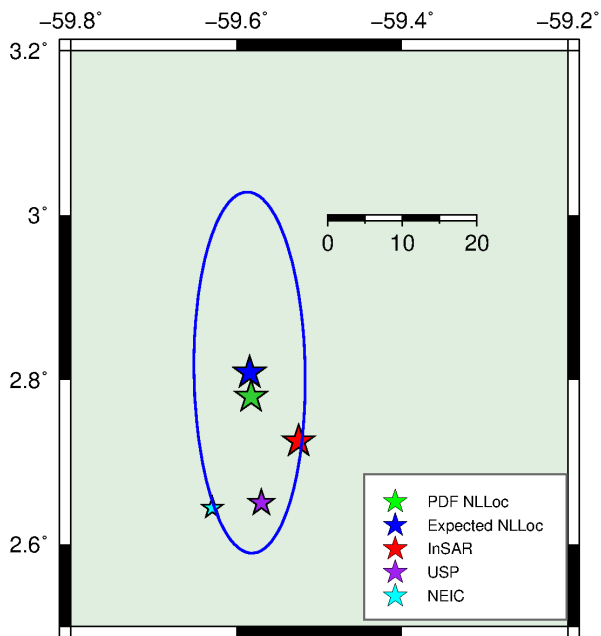


Figure 8: Guyana earthquake relocation using the 3D velocity model and NLLoc routine. Red star is the best epicenter given by InSAR (Assumpção et al., 2021). Purple and blue stars are RSBR and USGS/NEIC locations.

## Conclusions

The elaborated 3D velocity model shows a realistic velocity variation incorporating important interfaces, such as sedimentary basement, Moho depths, the Nazca slab (when is pertinent), and the global mantle discontinuities at  $\sim 420$  and  $\sim 660$  km.

Using our 3D velocity model, we have successfully relocated the well-known Aiquile earthquake, as well as two events recorded on the platform by RSBR: the 2020 Amargosa event and the 2021 Guyana earthquake. However, larger uncertainties are found when higher azimuthal gaps exist, and the stations are far away from the event.

We suggest that the next steps would be the construction of an S-wave counterpart model, test it with more local events, specially in the platform and try to accommodate the location of Andean events recorded by the RSBR network. Unfortunately no well settled GT event was recorded by the RSBR so far, the recent Guyana earthquake is under study by the USP/RSBR seismological group and it is a candidate to be the 1st GT event well recorded by the RSBR.

## Acknowledgments

The authors would like to thank the support from the CNPq agency for the scholarship of C.R.V, and the support of the FUSP and Institute of Astronomy, Geophysics and Atmospheric Sciences (IAG) by the financial support to develop most of this work in the Geoazur Laboratory in France.

## References

- Assumpção M., Ardito J., Barbosa J. R., An improved velocity model for regional epicentre determination in Brazil. In IV Simpósio Brasileiro de Geofísica, 2010, p. cp
- Assumpção M., Calhau J., Rosa D., Bianchi M., Baksh J., Assing D., Basdeo C., October S., Persaud L., Dias F., Jolivet R., Calais E., The M 5.7 earthquake of 31-January-2021, Guyana: preliminary field results of the largest recorded earthquake in the Guyana Shield, northern Amazon craton, Seismic Record of Seismological Society of America, 2021, *Submitted*.
- Beck S., Zandt G., The nature of orogenic crust in the central Andes, *Journal of Geophysical Research - Solid Earth*, 2002, vol. 107
- Béthoux N., Theunissen T., Beslier M.-O., Font Y., Thouvenot F., Dessa J.-X., Simon S., Courrioux G., Guillen A., Earthquake relocation using a 3D a-priori geological velocity model from the western Alps to Corsica: Implication for seismic hazard, *Tectonophysics*, 2016, vol. 670, p. 82
- Bianchi M. B., Assumpção M., Rocha M. P., Carvalho J. M., Azevedo P. A., Fontes S. L., Dias F. L., Ferreira J. M., Nascimento A. F., Ferreira M. V., Costa I. S. L., The Brazilian Seismographic Network (RSBR): Improving Seismic Monitoring in Brazil, *Seismological Research Letters*, 2018, vol. 89, p. 452
- Bondár I., Storchak D., Improved location procedures at the International Seismological Centre, *Geophysical Journal International*, 2011, vol. 186, p. 1220
- Christensen N. I., Mooney W. D., Seismic velocity structure and composition of the continental crust: A global view, *Journal of Geophysical Research: Solid Earth*, 1995, vol. 100, p. 9761
- Damodara N., Rao V. V., Sain K., Prasad A., Murty A., Basement configuration of the West Bengal sedimentary basin, India as revealed by seismic refraction tomography: its tectonic implications, *Geophysical Journal International*, 2017, vol. 208, p. 1490
- de Lima M. V. A., Stephenson R. A., Soares J. E. P., Fuck R. A., de Araújo V. C., Lima F. T., Rocha F. A., Characterization of crustal structure by comparing reflectivity patterns of wide-angle and near vertical seismic data from the Parnaíba Basin, Brazil, *Geophysical Journal International*, 2019, vol. 218, p. 1652
- Font Y., Kao H., Liu C.-S., Chiao L.-Y., A comprehensive 3D seismic velocity model for the eastern Taiwan southernmost Ryukyu regions, *Terrestrial Atmospheric and Oceanic Sciences*, 2003, vol. 14, p. 159

## 3D VELOCITY MODEL FOR THE SOUTH AMERICAN PLATFORM

- Funning G. J., Barke R. M., Lamb S. H., Minaya E., Parsons B., Wright T. J., The 1998 Aiquile, Bolivia earthquake: A seismically active fault revealed with InSAR, *Earth and Planetary Science Letters*, 2005, vol. 232, p. 39
- Kennett B. L. N., Engdahl E., Traveitimes for global earthquake location and phases identification, *Geophysical Journal International*, 1991, vol. 105, p. 429
- Krishna V., Rao V. V., Processing and modelling of short-offset seismic refraction coincident deep seismic reflection data sets in sedimentary basins: an approach for exploring the underlying deep crustal structures, *Geophysical Journal International*, 2005, vol. 163, p. 1112
- Laske G., Masters G., Ma Z., Pasyanos M., Update on CRUST1.0 A 1-degree global model of Earth's crust. In *Geophys. res. abstr*, vol. 15, 2013, p. 2658
- Lin G., Three-Dimensional Seismic Velocity Structure and Precise Earthquake Relocations in the Salton Trough, Southern California, *Bulletin of the Seismological Society of America*, 2013, vol. 103, p. 2694
- Lomax A., Absolute Location of 2019 Ridgecrest Seismicity Reveals a Shallow Mw 7.1 Hypocenter, Migrating and Pulsing Mw 7.1 Foreshocks, and Duplex Mw 6.4 Ruptures, *Bulletin of the Seismological Society of America*, 2020, vol. 110, p. 1845
- Lomax A., Michelini A., Curtis A., Meyers R., Earthquake location, direct, global-search methods, *Encyclopedia of complexity and systems science*, 2009, vol. 5, p. 2449
- Molinari I., Argnani A., Morelli A., Basini P., Development and testing of a 3D seismic velocity model of the Po Plain sedimentary basin, Italy, *Bulletin of the Seismological Society of America*, 2015, vol. 105, p. 753
- Murty A., Sain K., Prasad B. R., Velocity structure of the West-Bengal sedimentary basin, India along the Palashi-Kandi profile using a travel-time inversion of wide-angle seismic data and gravity modeling—an update, *Pure and applied geophysics*, 2008, vol. 165, p. 1733
- Myers S., Begnaud M., Ballard S., Pasyanos M., Phillips W., Ramirez A., Antolik M., Hutchenson K., Dwyer J., Rowe C., Wagner G., A Crust and Upper-Mantle Model of Eurasia and North Africa for Pn Travel-Time Calculation, *Bulletin of the Seismological Society of America*, 2010, vol. 100, p. 640
- NOAA National Geophysical Center, 2009 Technical report ETOPO1 1 arc-minute global relief model. NOAA National Centers for Environmental Information
- Nugraha A. D., Shiddiqi H. A., Widiyantoro S., Thurber C. H., Pesicek J. D., Zhang H., Wiyono S. H., Ramdhan M., Wandono Irsyam M., Hypocenter Relocation along the Sunda Arc in Indonesia, Using a 3D Seismic-Velocity Model, *Seismological Research Letters*, 2018, vol. 89, p. 603
- Portner D. E., Rodríguez E. E., Beck S., Zandt G., Scire A., Rocha M. P., Bianchi M. B., Ruiz M., França G. S., Condori C., Alvarado P., Detailed Structure of the Subducted Nazca Slab into the Lower Mantle Derived From Continent-Scale Teleseismic P Wave Tomography, *Journal of Geophysical Research: Solid Earth*, 2020, vol. 125, p. e2019JB017884
- Rivadeneira-Vera C., Bianchi M., Assumpção M., Cedraz V., Julià J., Rodríguez M., Sánchez L., Sánchez G., Lopez-Murua L., Fernandez G., Fugarazzo R., Team T. -B. P., An Updated Crustal Thickness Map of Central South America Based on Receiver Function Measurements in the Region of the Chaco, Pantanal, and Paraná Basins, South-western Brazil, *Journal of Geophysical Research: Solid Earth*, 2019, vol. 124, p. 8491
- Sandrin A., Thybo H., Seismic constraints on a large mafic intrusion with implications for the subsidence history of the Danish Basin, *Journal of Geophysical Research: Solid Earth*, 2008, vol. 113
- Simmons N. A., Myers S. C., Johannesson G., Matzel E., LLNL-G3Dv3: Global P wave tomography model for improved regional and teleseismic travel time prediction, *Journal of Geophysical Research: Solid Earth*, 2012, vol. 117
- Soares J. E., Stephenson R., Fuck R. A., De Lima M. V., De Araújo V. C., Lima F. T., Rocha F. A., Da Trindade C. R., Structure of the crust and upper mantle beneath the Parnaíba Basin, Brazil, from wide-angle reflection–refraction data, *Geological Society, London, Special Publications*, 2018, vol. 472, p. 67
- Süss M. P., Shaw J. H., P wave seismic velocity structure derived from sonic logs and industry reflection data in the Los Angeles basin, California, *Journal of Geophysical Research: Solid Earth*, 2003, vol. 108
- Wu Y.-M., Chang C.-H., Zhao L., Teng T.-L., Nakamura M., A Comprehensive Relocation of Earthquakes in Taiwan from 1991 to 2005, *Bulletin of the Seismological Society of America*, 2008, vol. 98, p. 1471